Realistic application of short-lived fission product delayed neutron, gamma-ray analysis for simultaneous nondestructive trace quantification of U, Pu mixtures on cellulose swipes

David Glasgow[a,*], Ramkumar Venkataraman[a], Kayron Rogers[a], Brian Ticknor[a], Justin Knowles[b] Stephen Croft[c]

[a]*Oak Ridge National Laboratory, Oak Ridge, TN, United States*
[b]*Y12 National Security Complex, Oak Ridge, TN, United States*
[C]*Lancaster University, Lancaster, United Kingdom*
[*]*Corresponding author*

Abstract

Detection and characterization of fissile traces are of interest to the international nuclear nonproliferation community, including the International Atomic Energy Agency. Pre-inspection check samples are analyzed by neutron activation analysis at the High Flux Isotope Reactor operated by the Oak Ridge National Laboratory under the umbrella of the IAEA Network of Analytical Laboratories. The simultaneous quantification of U and Pu mixtures was accomplished using the combined delayed neutron (DN) delayed gamma-ray (DG) method to analyze cellulose swipes with actinide loading <1ng in a blind field trial. The total fissile quantity was measured by the DN counts and the relative proportions of U, Pu were determined by calibration of the ^{104}Tc / ^{141}Ba fission product count ratio using known mixtures. The DNDG method demonstrated high accuracy in flagging the presence of ^{239}Pu in uranium down to <100pg mass loading. Peak significance tests helped to control false positive Pu flagging and simultaneous quantification of U and Pu loading was accomplished on samples that passed the significance tests.

1. Introduction and background

The detection and characterization of fissile traces as various matrices are of significant interest to the International Atomic Energy Agency (IAEA) for international safeguards and nonproliferation assessments. For several years, Oak Ridge National Laboratory (ORNL) has participated in the IAEA Network of Analytical Laboratories (NWAL). NWAL serves the IAEA through the isotopic analysis of fissile traces in IAEA Environmental Samples with funding and direction from the National Nuclear Security Administration Office of International Safeguards (NA-241) and the U.S. Department of State. A wide range of techniques, from gamma-ray spectrometry to high-resolution mass spectrometry, are employed to accomplish the NWAL mission.

The primary goal of this work was to assess the ability of the delayed neutron delayed gamma (DNDG) method [1] to correctly flag the presence of Pu in U/Pu mixtures and single-component samples ranging from blank to 1,000 pg. In addition, the quantification of relative U and Pu amounts is desired where possible and was reported for samples with statistically measurable 191 keV (^{141}Ba) and 358 keV (^{104}Tc) gamma-rays.

1.1 Short-lived fission product analysis

Several groups have investigated short-lived fission products during the last couple of decades. Many have added new measurements of fission product yields from neutron-induced fission by thermal [2] and

fast [3, 4] neutrons. Time regimes ranging from seconds [5] to days [6] decay have been investigated for diverse purposes, including decay heat calculations, actinide identification [7, 8], and forensics applications [9, 10]. A few researchers, including our group, have examined fission product ratio analysis for simultaneously resolving actinide mixtures. [11, 12] Modeling and measurement of delayed neutron count rate curves have also been performed to address fissile actinide mixtures, with limited success.[13-15] Many of the delayed neutron rate curve measurements are overwhelmed by compounding uncertainty as the fissile quantity decreases to the trace levels of safeguards interest, however. We report the use of fission product ratios in a realistic field trial setting of relevant matrix, fissile material mass, and analysis scheme throughput and design to strengthen and expand on the existing analysis of pre-inspection check (PIC) samples that is already underway using NAA delayed neutron and delayed gamma techniques.

1.2 Application to IAEA PIC sample stream

Each year, the IAEA sends hundreds of cellulose swipes called *preinspection check* (PIC) samples for interrogation by NAA for uranium traces. PIC samples are taken from the inspectors themselves to ensure that they are free of contamination prior to conducting inspections at nuclear facilities. Two NAA measurements are currently performed after irradiation: DN counting for ^{235}U and DG counting for ^{238}U. The DNDG scheme adds a second DG count to facilitate Pu flagging and quantification by fission product measurement. Together, the method addresses ^{235}U, ^{238}U, 5/8 ratio, and plutonium presence and proportion to uranium, significantly improving and strengthening the PIC sample screening by NAA. Both techniques are performed using comparator analysis methods, which reduce the contributors to overall uncertainty by not requiring absolute detector efficiency calibration and by not using nuclear parameters like cross section, fluence rate measurement, decay branching, and fission product production variables.

The DNDG concept of operations (CONOPS) must fit within the existing protocol for analysis of IAEA PIC samples for maximum utility. After all samples are analyzed for ^{235}U and the DN counts are recorded, samples that meet the action level are irradiated again to generate ^{239}Np for ^{238}U measurement. Because of the nature of the cellulose paper of the J-swipes, 4–5 days of cooling are required for reduction of the ^{24}Na that is produced in the swipe matrix. The DG fission product measurements were designed to occur after the second irradiation, with only 20 minutes of cooling. In this way, the current cycle of irradiating, decay, and counting is sufficient with the addition of another gamma count in the middle to add plutonium flagging.

1.3 Low-Mass / High Mass fission product ratio calculation and theory

Mathematically, the DNDG process is easy to understand and estimate uncertainties.[1] The capability to distinguish between two different fissile species, i.e., ^{235}U and ^{239}Pu in the sample, stems from the fact that the fission yields for high mass number (>120) fission products for the odd mass-numbered actinides are very similar, whereas the yields for the low mass (<120) fission products vary significantly (Figure 1). The ratio of suitable low mass to high mass fission product yields, determined using gamma spectrometry, can then be used to uniquely flag the presence of an odd mass-numbered actinide, e.g., ^{239}Pu, in a binary mixture of ^{235}U and ^{239}Pu. The primary objective of the DNDG method is to flag the presence of ^{239}Pu in the sample. Additionally, quantification of ^{239}Pu and ^{235}U by combining DN and DG results can be done. The low and high mass fission products that were amenable for measurements were ^{104}Tc and ^{141}Ba. ^{104}Tc has a high yield for ^{239}Pu, whereas the yield of ^{141}Ba is approximately the same for ^{235}U and ^{239}Pu. Because the measurement is compared to a known standard, and the half-lives of the fission products ^{104}Tc and ^{141}Ba are approximately the same, the net peak counts in the gamma-ray peaks may be used for calculation rather than the saturated activity. The gamma-ray peaks employed are 358 keV and 190 keV of ^{104}Tc and ^{141}Ba, respectively. The peak area ratio (R) can be written as follows.

$$R = \frac{a_4 \cdot U + b_4 \cdot P}{a_1 \cdot U + b_1 \cdot P} \quad (1)$$

In equation 1, a_4 and a_1 are the ^{104}Tc and ^{141}Ba net peak areas from ^{235}U fission, respectively, and b_4 and b_1 are the ^{104}Tc and ^{141}Ba net peak areas from ^{239}Pu, respectively. U and P are the mass values for ^{235}U and ^{239}Pu. Equation 1 may be rewritten in terms of the Pu fraction (X) expressed as $P/(U+P)$ as shown.

$$R = \frac{(a_4/a_1) \cdot (1-X) + (b_1/a_1) \cdot (b_4/b_1) \cdot X}{(1-X) + (b_1/a_1) \cdot X}, 0 < X < 1 \quad (2)$$

Normalizing the ratio R with respect to U-only samples and designating $Y = \frac{R}{(a_4/a_1)}$, equation (2) can be rewritten as follows.

$$Y = \frac{(1-X) + c \cdot d \cdot X}{(1-X) + c \cdot X} \quad \text{where, } c = b_1/a_1 \text{ and } \quad \frac{(b_4/b_1)}{(a_4/a_1)} = d \quad (3)$$

Solving equation 4 for X, we arrive at the ^{239}Pu fraction (equation 4).

$$X = \frac{(Y-1)}{(Y-1) + c \cdot (d-Y)} \quad (4)$$

To determine the ^{239}Pu fraction, X, a few calibration parameters must be measured in addition to the peak areas for the binary mixtures. The calibration parameters are (i) the ratio of the net peak areas a_4/a_1 based on a U-only standard; (ii) the ratio of net peak areas b_4/b_1 based on a Pu-only standard; (iii) the parameter d, which is the double ratio given in equation (3); and (iv) and the parameter c, which is the ratio of ^{141}Ba peak areas for single-actinide U and Pu standards. The uncertainty in the Pu fraction, X, may be calculated using standard error propagation formulas and is driven by counting statistics and weighing uncertainty components.

2. Experiment Methodology

The sample material used in this work was a cellulose swipe marketed by Chiyoda Technol Corporation of Tokyo, Japan and is sold under the part number E0803004. All samples and standards were prepared on this substrate, nicknamed "J-Swipe," and pictured in Figure 2. The wings are removed at the perforated line and the center portion was folded to fit in the irradiation containers (rabbits). After irradiation, the sample was removed from the rabbit, placed in a 4 mL Wheaton® Omni-Vial™, and pressed flat by introduction of a plastic test tube plug to produce a regular counting geometry approximately 10mm diameter and 5 mm height in the bottom of the vial.

2.1 Fluence rate monitoring

The irradiation of the test samples and standards was conducted over three consecutive days in order to acquire the results on a single detector. Each day, a fluence rate monitor was irradiated and counted to determine the thermal and epithermal fluence rates. Aluminum foils containing Mn (0.0879%) and Au (0.100%) were irradiated 20 seconds and counted on axis, 30cm from the detector after several hours of decay. The cross section of ^{55}Mn(n,γ)^{56}Mn monitor reaction follows 1/v shape, where v is neutron speed, and samples the thermal part of the spectrum. The ^{197}Au(n,γ)^{198}Au monitor reaction has a strong resonance feature in the epithermal energy range and is used to estimate the epithermal spectrum portion. Table 1 documents the monitor masses and thermal and epithermal fluence rate results for each day. Since

this work utilizes peak count rate ratios, rather than absolute count rates, the fluence rate values are not used to calculate results. However, they do show the stability of the irradiation position during the measurement campaign.

2.2 Calibration Standards and Mixtures

Calibration standards and mixtures were prepared by Glasgow and Venkataraman using well-characterized actinide standards. Uranium calibration was provided by analysis of National Institute of Standards and Technology (NIST)-traceable uranium standards derived from High Purity Standards® 1,000 ppm uranium calibration solution (lot 1014018) that had been gravimetrically diluted and aliquoted onto the calibration swipes. Plutonium calibration was provided by analysis of gravimetrically diluted certified reference materials CRM-137 and IRMM-086. Blanks composed of clean J-swipes were analyzed for blank subtraction, especially during the delayed neutron analysis phase. Uranium–plutonium mixtures were also prepared and analyzed using the standards described above. One of the actinides was pipetted onto the substrate, allowed to dry under dry air purge overnight and the second actinide was added the following day and similarly dried. Weighing was performed on a Mettler-Toledo® XPE206™ microbalance that was calibrated by ORNL Metrology and verified by calibrated check weights that bracketed the sample weights at each weighing event. Acid degradation of the cellulose paper was observed in some samples and standards, making a few of the materials unusable because the swipe could not be reliably recovered from the rabbit. Those occurrences are marked in the data results tables.

2.3 Test (field) Samples

Test samples were prepared by Rogers and Ticknor, and the mass values, isotopic abundances, and compositions were withheld from Glasgow and Venkataraman until the results from the analysis were reported and finalized. In this way, the analysts were blind to the composition. Mass values 0.0 – 1000 pg were the limits for uranium and plutonium content and a total of 35 samples were prepared, including U-only, Pu-only, and blank samples. The sample identifiers were also randomized for additional information security during the analysis phase. The Pu and U master solutions were chosen from low-uncertainty materials with well-known isotopic composition and included certified reference materials, materials characterized by round-robin, or in-house working reference materials. The uranium solution had been previously characterized by Davies and Gray titration and the plutonium solution was spiked with ultra-pure ^{244}Pu and analyzed by mass spectrometry.

Serial dilutions without mixing were made of each of the master U and Pu solutions so that the weight of the solution to be loaded would be in the range of approximately 50–180 mg. J-swipes were folded and then placed into rabbits, which were held in small disposable cups. The numerical label was applied to the cups as means of identification because the rabbits could not be altered. The rabbits with J-swipes were individually placed onto a balance readable to 0.01 mg, the balance was zeroed, the appropriate solution was loaded with a pipet directly onto the J-swipe and the weight was recorded. The uranium solution was loaded first and then dried overnight in a HEPA filtered box with a fan and following day, the plutonium solution was loaded and again dried overnight.

2.4 Delayed neutron analysis

All samples and standards were irradiated in the High Flux Isotope Reactor PT-2 pneumatic transfer system that accesses the outer edge of the reactor permanent beryllium reflector.[16] This pneumatic tube exhibits typical fluence rate of 4.0E+13 n cm^{-2} s^{-1} that is highly thermalized such that ^{238}U fast fission rate is very low. Modeled fission rates for ^{235}U, ^{239}Pu, and ^{238}U are 6.9E+7, 9.3E+7, and 320 fissions s^{-1} μg^{-1}, respectively, according to ORIGEN [17] used as detailed in section 2.6 below. The irradiations were 180 s followed by a 5 s decay and 60 s counting in the ^{3}He detector array that is in-line with the sample transfer system. The detector array is populated with 18 ^{3}He tubes having 50 mm diameter, 30 cm active

length and 5 atm fill pressure resulting in an overall detection efficiency of about 35% for delayed neutrons. All materials were allowed to decay overnight before the delayed gamma-ray analysis step such that the ^{141}Ba and ^{104}Tc formed during the delayed neutron analysis step were completely gone.

2.5 Delayed gamma analysis

Following the analysis protocol for actual IAEA PIC samples, irradiation of the test samples and standards was conducted the day following the DN analysis. Samples that exhibited acid degradation were rejected after irradiation because they presented challenges for recovery of the swipe. Irradiations occurred in the PT-1 irradiation facility for 5 min followed by about 10 min decay prior to opening the rabbit. The typical fluence rate (Table 1) in the PT-1 facility is approximately an order of magnitude higher than in the PT-2 facility which greatly improves the sensitivity limits of DG analysis. Samples were retrieved and placed in counting vials as described in Section 2.0 above. A total of 20 min was allowed to expire between the end of irradiation and the start of count and counting for 30 min occurred at 20 cm shelf height. The high purity germanium (HPGe) detector was an ORTEC® GMX™ having a 58% relative efficiency and was operated using the Canberra® Genie2000™ MCA software under loss-free counting conditions,[18] employing the Canberra® Lynx™ digital spectroscopy analyzer. The gamma-ray spectra were analyzed using PeakEasy™ regions of interest (ROI) gamma analysis software.[19] The same ROI were applied to each spectrum and included 8 background channels on either side of the peak ROI. Count rate averages for both the peaks and continuum under the peak were calculated and the continuum was then subtracted.

2.6 Modeling, simulation, and data processing

The U and Pu calibration samples were modeled along with a few mixtures using the ORIGEN module of the SCALE nuclear depletion code.[17] The PT-1 neutron spectrum shape and magnitude were taken from previous activation wire experiments, MCNP simulations, and the daily fluence rate monitors. In addition, the regions of interest were assessed for statistical significance by examining sample 14, which was judged to be a blank according to the DN counts, which were not significantly different from known blanks. The net counts for the 190 keV (^{141}Ba) and 358 keV (^{104}Tc) regions of interest were 1374 and 1185, respectively, which may be used as inputs to the Currie formalism [20] to calculate a limit of quantitation. The limit of quantitation is 14.1 times the background and corresponds to the case in which the background is not well known, as postulated by Currie. Results that fail to meet the significance test are reported as delayed neutron results only. In this way, the presence of Pu may be flagged even in cases in which the peak statistics are too poor to calculate Pu quantity. This may be summarized in the following selection rules:

1. If either or both the 190 keV or 358 keV peaks failed the sensitivity test, the fissile quantity was reported from the U equivalents derived from the DN data.
2. In cases when both ROIs passed the sensitivity test, the U/Pu ratio was calculated using the comparator factors and applied to the DN data to parse the total fissile quantity into U, Pu bins.
3. If the 358 keV peak was statistically significant, the presence of Pu was flagged in the sample because ^{104}Tc is much more sensitive to Pu fission than U fission.

Comparator factors were derived from the ROI ratios for single-element standards and were used to calculate quantitative results when the selection rules were met.

3. Results and Discussion

DN data were acquired for all samples. However, samples 1, 7, 10, 21, and 34 were not analyzed by the delayed gamma DG method. Samples 1, 10, and 34 were badly acid degraded and samples 7, 21 were obviously blanks according to the DN results and were not analyzed further.

3.1 Modeling versus measured Ratio

The ORIGEN modeled $^{104}Tc/^{141}Ba$ ratio calculated from JEFF 3.0 [21] fission product data was compared to the experimentally measured ratio for the calibration materials and is presented in Figure 3. The two sets of data have essentially identical shapes, as evidenced by the polynomial fit. However, the measured data display about 25% positive bias over the model. Some possibilities for explaining the bias seem apparent. The first is that the 190 keV peak may be interfered and have counts that are correspondingly too high. Indeed, that peak is broad and has a shoulder on the high-energy side which may indicate some ^{101}Mo at 191.9 keV is present in the ROI for ^{141}Ba. However, since ^{141}Ba originates from I/Xe volatile fission products, some losses may be expected and would work to temper the effect of the ^{101}Mo contribution to the ROI. ^{104}Tc is formed from nonvolatile fission products and is not expected to have volatile losses. However, ^{83}Se emits at 356.7 keV and could contribute to the ^{104}Tc region of interest. Although the precursors to ^{141}Ba in the mass 141 chain are short-lived and completely decayed away prior to opening the irradiation container, the volatile ^{141}I and ^{141}Xe may not have remained in the sample matrix and thus would not be present in the sample that was transferred for counting. Loss of the volatile precursors may be the best explanation for the model / measured discrepancy. Nevertheless, the shape of the measured values is correctly predicted by the model.

3.2 Delayed Neutron (DN) results

The total fissile quantity present in the samples was measured by delayed neutron counting. Table 2 shows the results for DN counting, uncertainties, and comparison to the true total fissile mass values derived from the sample loading recipe. Because both the temporal distribution of delayed neutron precursors and the number of precursors per fission vary by actinide, discrimination of unknown mixtures of U and Pu is a challenge. This is especially true at the low fissile quantities that are relevant to PIC samples. Such low quantities resulted in decay curves that had enough scatter to confound mathematical fitting without significant uncertainties. Inspection of Table 2 reveals which samples are mostly U and which are mostly Pu because the recovery accuracy decreased as the U/Pu ratio decreased. Despite the higher fission cross section for ^{239}Pu, fewer delayed neutrons are emitted. This results in approximately three times more sensitivity for ^{235}U than for ^{239}Pu by delayed neutron counting, as evidenced by Table 2.

3.3 Plutonium flagging and peak significance

An important consideration for IAEA is whether there is any indication that a sample may have ^{239}Pu rather than only U. For a sample to exhibit positive detection of the 358 keV peak, and thus Pu, the signal to background ratio must be at least 14.1. Similarly, for U detection, the 191 keV peak must meet that criterion. Table 3 reveals the results of the peak significance tests, Pu flagging results, and the calculation method for results according to the selection rules in section 2.6 above. Recall from section 2.6 that if either peak fails the significance criterion, the DN counts are assigned to U and reported as fissile equivalents. However, Pu presence may be flagged if the ^{104}Tc (358 keV) passes its significance test even if the ^{141}Ba (191) does not. Of the 25 samples that contained Pu and were analyzed, 19 were correctly flagged for Pu presence. Even for Pu quantity below 100 pg, six of the nine samples were correctly flagged and the remaining three (2, 13, 17) were all below 50 pg and potentially indicates a sensitivity limit for Pu flagging. On the other hand, Pu presence was incorrectly flagged for samples 22, 38 and 40, which did not contain Pu. The false positive flagging of Pu is not desirable and could trigger application of mass spectrometric assets to analyze these or archived duplicate PIC samples to investigate. Figure 4

shows portions of four gamma-ray spectra, one for a 5 ng calibration sample and the others for samples 22, 38, and 40. There is a small peak evident at 358 in samples 22 and 40 that could result in a statistically allowed false positive for Pu flagging under the conditions of the peak sensitivity tests. Sample 40 shows more structure in the spectrum baseline in the 358 keV region that results in lower subtracted baseline counts, particularly on the lower energy side. In addition, the spectrum baseline is much higher for all three samples for the calibration sample, despite having much lower uranium content. This baseline elevation was caused by a small amount of sodium impurity, of unknown origin, in the uranium standard used to prepare the samples. The increased count rate also led to resolution degradation which could cause calibration errors if a shape calibration was used to reduce the spectra. However, Figure 4 shows the ROI analysis boundaries were sufficient to accommodate the resolution changes without losing counts on the peak edges. The remaining Pu-free samples, 14, 18, 28, 30, and 36 correctly failed the peak sensitivity test for the 358 keV peak of the Pu-sensitive ^{104}Tc. Sample 18 is similar to 40 in that it contained 500 pg ^{235}U and may indicate that the sensitivity test itself was well-optimized between null Pu rejection and false positive incidence. Samples 14, 28, and 36 contained neither U nor Pu.

In the U sensitivity results, of the 31 samples that contained U and were analyzed, 22 were correctly judged on peak significance. Sample 18, which contained 500 pg ^{235}U but failed the sensitivity test was unusual, for which there is no explanation outside of the random statistics or baseline perturbation around the 191 keV peak. The remainder had either very low amounts <50 pg or were blanks that were loaded with significant Pu, >500 pg. The latter may have detectable ^{141}Ba and would benefit from the absence of Na impurity. The situation in which a PIC sample is composed solely of Pu is rare, owing to the purpose and manner of collection.

3.4 Plutonium, Uranium quantification results as DNDG

The primary purpose of the DNDG method was to select samples that indicated Pu presence in order to target mass spectrometric analysis assets. Once flagged, Pu quantification was possible for some samples. Figures 5 and 6 present the results for U, Pu quantification using the DNDG method. Generally, the Pu results (Figure 5) showed that for 60% of the samples, the calculated Pu quantity was within 20% of the recipe value. Of the six samples that had recoveries above 20% absolute variance, three contained less than 75 pg Pu. The remaining samples did not follow a trend. The lower mass limit for usability of the DNDG method to calculate Pu is about 100 pg. Figure 6 contains the uranium results along with the uranium equivalents calculated from the DN data without performing DNDG calculations. These data appear to suggest an overall negative bias, particularly as the U quantity increases, but the results were generally within 20% absolute error with larger deviation below 100 pg. For both actinides, when samples were composed solely of one component, the DNDG method assigned more counts to the minority isotope than warranted.

3.5 Performance on blanks

Actinide-free blank samples are easily identified by the DN results alone. However, when one actinide is present, DN counting alone cannot be used to identify the actinide. Overall, all of the no-actinide blanks were correctly identified and more of the U-only blanks were correctly identified than the Pu-only blanks. A detailed analysis of additional blank samples may improve indicators that could be useful for detecting low levels of actinide, where most of the blank errors occurred.

4. Conclusions

The DNDG method worked well in estimating the actinide proportion for U, Pu when the peak significance tests were successful. Performance on blank rejection and, to a greater extent, Pu flagging

was even better. Designed as expanded capability that fits withing the analytical scheme for PIC samples by NAA, the DNDG method adds valuable characterization information without interfering with or delaying the flow of events, thus fitting into the existing CONOPS. DNDG does not require additional reactor irradiation, any preparatory or separations chemistry, and is sensitive enough to be applied to PIC sample analysis at the tens of picogram level. There is an increased, but manageable, radiological contamination risk when employing DNDG simply because the decay time before opening the rabbit and handling the sample is much reduced. Acid degradation of the sample material was observed to negatively impact the analyses and could be mitigated by freshly preparing calibration materials. There occurred an unexpected reactor startup delay that produced additional damage to the cellulose matrix during this work.

More work is needed to develop higher method reliability for very low actinide levels, < 100 pg. Although the selection criteria strike about the right balance between false positive and negative results, the importance of that balance warrants additional experiments to generate higher data populations to better refine the significance tests. The method indicated the presence of Pu better when U, Pu mixtures were investigated and did have some false positive indications when only one actinide was present. The gamma-ray spectra will be evaluated to determine if additional fission products are present that could inform the sample composition and assist with decision making for data reduction. For example, ^{94}Y is detected in our calibration standard spectra and has been identified [11] as sensitive to U/Pu discrimination. During this work all uncertainties were propagated through to yield realistic total error budgets but fine tuning the uncertainties in future work could lead to fewer false positive results.

5. Acknowledgement

The authors gratefully acknowledge the National Nuclear Security Administration Office of International Safeguards for funding this research and for their very helpful manuscript technical review.

6. References

[1] Venkataraman, R., Glasgow, D., Croft, S., and Knowles, J., Nondestructive co-assay of U and Pu fissile traces by combined delayed neutron and delayed gamma fission product neutron activation analysis," in Proceedings of the INMM and ESARDA Joint Virtual Annual Meeting, August 23-26 and August 30-September 1, 2021.

[2] S. Stave, A. Prinke, L. Greenwood, D. Haas, J. Burke, J. Ressler, A. Tonchev, W. Younes, Reducing uncertainties for short-lived cumulative fission product yields, J. Radioanal. Nucl. Chem. 307 (2016) 2221-2225.

[3] E. Finn, L. Metz, L. Greenwood, B. Pierson, J, Friese, R. Kephart, J. Kephart, Short-lived fission product measurements from >0.1 MeV neutron-induced fission using boron carbide, J. Radioanal. Nucl. Chem. 293 (2012) 267-272.

[4] B. Pierson, A. Prinke, L. Greenwood, S. Stave, R. Wittman, J. Burch, J. Burke, S. Padgett, J. Ressler, G. Slavik, A. Tomashiro, A. Tonchev, W. Younes, Improved cumulative fission yield measurements with fission spectrum neutrons on ^{235}U, Lawrence Livermore National Laboratory (2019) LLNL-JRNL-783000.

[5] A. Demidov, L, Govor, I, Mikhailov, Use of gamma radiation from short-lived fission products for detecting ^{235}U and ^{239}Pu, Atomic Energy 98 (2005) 347-351.

[6] S. Biegalski, N. Kane, J. Mann, T. Tipping, K, Dayman, Neutron activation of NIST surrogate post-detonation urban debris (SPUD) candidate SRMs, J. Radioanal. Nucl. Chem., 318 (2018) 187-193.

[7] R. Firestone, G. English, J. Reijonen, F. Gicquel, K-N. Leung, D. Perry, G. Garabedian, B. Bandong, Zs. Revay, G. Molnar, Analysis of fissile materials by high-energy neutron-induced fission decay gamma-rays, J.Radioanal. Nucl. Chem. 265 (2005) 241-245.

[8] D. Beddingfield, F. Cecil, Identification of fissile materials from fission product gamma-ray spectra, Nucl. Instr. and Meth. in Phys. Res. A, 417 (1998) 405-412.

[9] L. Metz, R. Payne, J. Friese, L. Greenwood, J. Kephart, B. Pierson, Experimental measurements of short-lived fission products from uranium, neptunium, plutonium, and americium, J. Radioanal. Nucl. Chem. 282 (2009) 373-377.

[10] M, Tohamy, J. Crochemore, K. Abbas, S. Nonneman, Identification of short-lived fission products in delayed gamma-ray spectra for nuclear material signature verifications, Nucl. Instr. Meth. in Phys. Res. A 978 (2020) 164347.

[11] R. Marrs, E. Norman, J. Burke, R. Macri, H. Shugart, E. Browne, A. Smith, Fission product gamma-ray line pairs sensitive to fissile material and neutron energy, Nucl. Instr. and Meth. in Phys. Res. A, 592 (2008) 463-471.

[12] J. Knowles, S. Skutnik, D. Glasgow, R. Kapsimalis, A generalized method for characterization of ^{235}U and ^{239}Pu content using short-lived fission product gamma spectroscopy, Nucl. Instr. and Meth. in Phys. Res. A, 833 (2016) 38-44.

[13] M. Sellers, D. Kelly, E. Corcoran, An automated delayed neutron counting system for mass determinations of special nuclear materials, J. Radioanal. Nucl. Chem. 291 (2012) 281-285.

[14] Kapsimalis, R., Glasgow, D., Anderson, B., Landsberger, S., The simultaneous determination of ^{235}U and ^{239}Pu using delayed neutron activation analysis, J. Radioanal. Nucl. Chem. (2013) published online.

[15] Li, X., Henkelmann, R., Baumgartner, F., Rapid determination of uranium and plutonium content in mixtures through measurement of the intensity-time curve of delayed neutrons, Nucl. Instr. Meth. in Phys. Res. B 215 (2004) 246-251.

[16] HFIR Reactor Overview, available at High Flux Isotope Reactor Technical Parameters | Neutron Science at ORNL (accessed April 28, 2023).

[17] W. A. Wieselquist, R. A. Lefebvre, and M. A. Jessee, Eds., SCALE Code System, ORNL/TM-2005/39, Version 6.2.4, Oak Ridge National Laboratory, Oak Ridge, TN (2020).

[18] G. P. Westphal, "Loss Free Counting—A concept for real-time compensation for dead-time and pile-up losses in nuclear pulse spectroscopy," Nucl. Instr. Meth. in Phys. Res. 146 (1977) 605-606.

[19] Rooney, B., Garner, S., Felsher, P., Karpius, P., (2015), PeakEasy 4.80 [Computer Program], Los Alamos National Laboratory, Release LA-CC-13-040, https://PeakEasy.lanl.gov

[20] L. Currie, "Limits for Qualitative Detection and Quantitative Determination: Application to Radiochemistry," Anal. Chem., 40(3) (1968) 586–593.

[21] NEA (2005), The JEFF-3.0 Nuclear Data Library, OECD Publishing, Paris

[22] Nuclear Data Sheets (2011), 112 (12), 2887-2996 https://doi.org/10.1016/j.nds.2011.11.002.

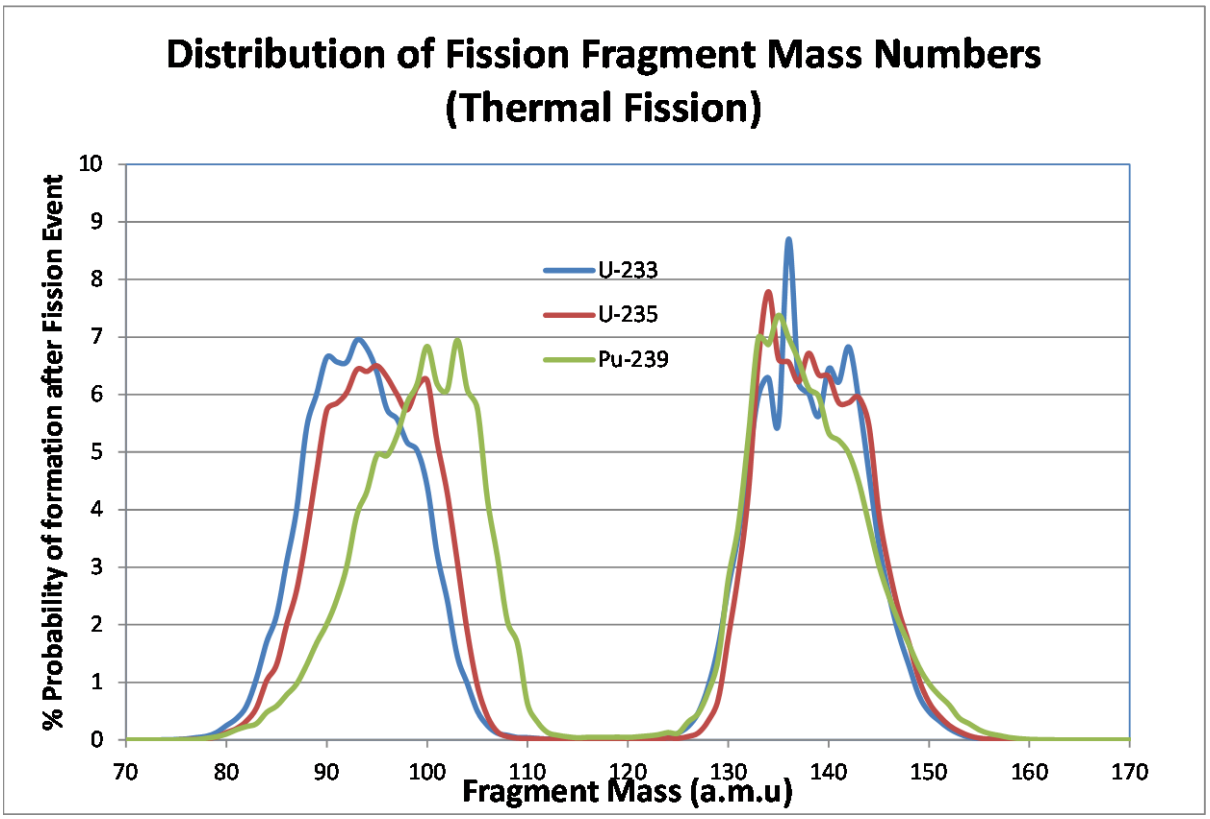

Figure 1. Thermal fission product probability distribution as a function of mass showing regions of large U/Pu fission product population differences (104-109 masses) and masses in which the fission product distributions are about the same (130-140). Data are taken from Nuclear Data Sheets volume 112 (12) pages 2887 - 2996 https://doi.org/10.1016/j.nds.2011.11.002.

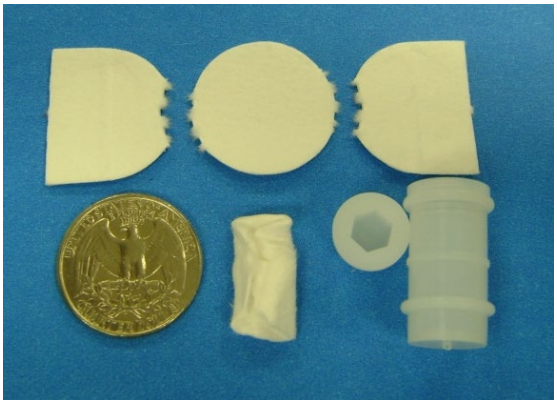

Figure 2. The cellulose J-Swipe paper is shown along with the polyethylene irradiation container "rabbit". For IAEA PIC sample applications, only the center disk is used.

Table 1. Presented are the fluence rate daily results during the measurement period. These are derived from gamma-ray measurements of the activated thermal (Mn) and epithermal (Au) monitors performed on each day of irradiations.

Date	Thermal fluence rate	Thermal/epithermal ratio
Day 1	4.302E + 14 n cm^{-2} s^{-1}	39.14
Day 2	4.227E + 14 n cm^{-2} s^{-1}	38.25
Day 3	4.222E + 14 n cm^{-2} s^{-1}	38.09

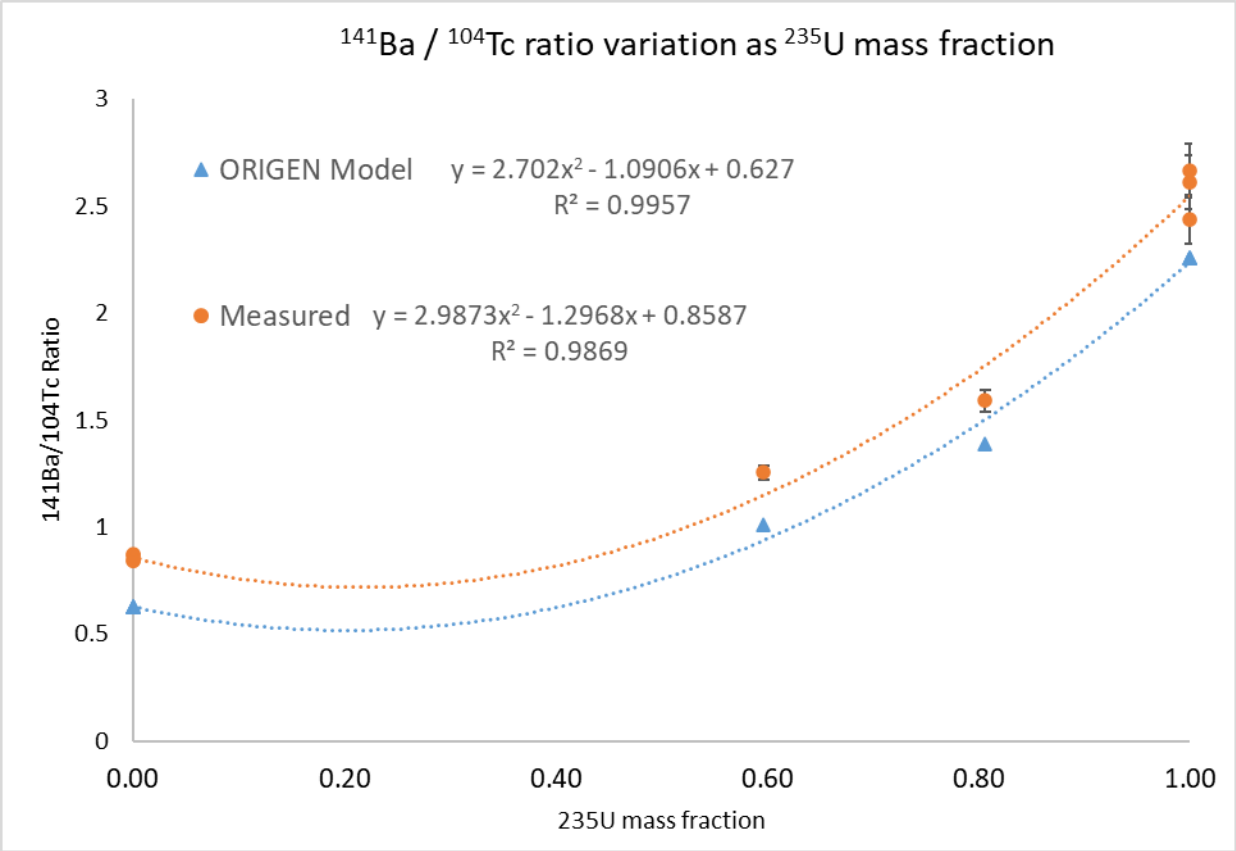

Figure 3. Shown are the modeled ^{141}Ba / ^{104}Tc ratios using ORIGEN (▲) and measurement (●) data for single and mixed actinide calibration standards. The fit data were second order polynomials. In all cases, the total fissile mass was 5 ng so when the ^{235}U mass fraction is 1.0, no Pu was present and, when the ^{235}U mass fraction is 0.0, the standard is composed solely of Pu. The shapes of the two curves are very similar and the offset between them may be caused by the combined effects of loss of volatile I, Xe precursors in the ^{141}Ba, interferences at the 191 keV peak of ^{141}Ba and the 356 keV peak of ^{104}Tc, and uncertainties in fission yield. Uncertainties in the measured values are depicted at the k=2 level and are obscured by the data point marker at 0.0 ^{235}U mass fraction.

Table 2. Presented are the total fissile quantities derived from the DN counting results. These are compared to the gravimetric total fissile loading from the preparation recipes. As expected, the accuracy of the DN quantification depends on the isotopic purity. Pure U samples (10, 18, 22, 30, 38, and 40) all exhibited excellent recovery where the recovery for pure Pu samples (11,15, 23, 25, 27, 29) was worse, owing to the differences in DN production between the two actinides.

Sample	^{235}U DN (pg)	$k = 2$ uncert	Total Fissile, pg	Expected ^{235}U, pg	Expected Pu, pg	Recovery (%)
1	195.7	34.5	250	63	187	78
2	47.4	32.3	49	25	24	96
3	221.8	34.9	251	190	61	88
4	659.7	40.7	752	567	186	88
5	601.5	39.9	749	379	370	80
7	−1.0	31.6	**0**	0	0	—
10	701.9	41.2	761	761	0	92
11	67.8	32.6	97	0	97	70
12	409.6	37.5	500	252	248	82
13	42.5	32.2	50	38	12	85
14	−5.2	31.5	**0**	0	0	—
15	165.9	34.1	248	0	248	67
16	832.8	42.7	1013	507	506	82
17	95.1	33	100	76	24	95
18	514.4	38.8	508	508	0	101
21	−3.2	31.5	**0**	0	0	—
22	240.4	35.2	256	256	0	94
23	739.1	41.6	999	0	999	74
25	41.7	32.2	49	0	49	86
26	47.9	32.3	50	13	37	97
27	357.9	36.8	506	0	506	71
28	−8.7	31.4	**0**	0	0	—
29	531	39.1	752	0	752	71
30	101.1	33.1	102	102	0	100
31	765.2	41.9	1007	252	755	76
32	561.6	39.4	753	189	564	75
33	373.5	37	495	126	369	75
34	446.6	38	500	379	122	89
35	902.6	31.3	999	752	246	90
36	1.7	9	**0**	0	0	—
37	71.8	12.3	98	25	73	73
38	45.2	11.1	51	51	0	88
39	72	12.3	99	51	48	73
40	944.5	31.9	1014	1014	0	93
41	194	16.5	248	126	122	78

Table 3. Peak Significance Results and Pu Flagging. Also summarized is the analysis mode used to derive the results. Total Fissile refers to results employing only the DN measurement, either because one or both sensitivity tests failed or because the sample was not analyzed.

Sample	Notes	S/s_B 190.0	S/s_B 358.0	Pu Flagged?	Expected Pu, pg	Derived Result
1	Sample not analyzed	—	—	N/A	187	Total Fissile
2	Both sensitivity tests fail	**8.0**	**11.3**	No	24	Total Fissile
3		14.7	14.5	**Yes**	61	DNDG
4		39.5	31.9	**Yes**	186	DNDG
5		42.6	43.3	**Yes**	370	DNDG
7	Sample not analyzed	—	—	N/A	0	Total Fissile
10	Sample not analyzed	—	—	N/A	0	Total Fissile
11	U sensitivity test fails	**11.7**	19.6	**Yes**	97	Total Fissile
12		32.6	31.3	**Yes**	248	DNDG
13	Both sensitivity tests fail	**9.4**	**13.0**	No	12	Total Fissile
14	Both sensitivity tests fail	**6.3**	**10.5**	No	0	Total Fissile
15		24.7	28.8	**Yes**	248	DNDG
16		51.1	50.4	**Yes**	506	DNDG
17	Pu sensitivity test fails	14.5	**12.0**	No	24	Total Fissile
18	Both sensitivity tests fail	**12.5**	**10.9**	No	0	Total Fissile
21	Sample not analyzed	—	—	N/A	0	Total Fissile
22		15.3	17.3	**Yes**	0	DNDG
23		38.0	52.2	**Yes**	999	DNDG
25	U sensitivity test fails	**10.7**	15.7	**Yes**	49	Total Fissile
26		13.4	15.3	**Yes**	37	Total Fissile
27		35.9	46.3	**Yes**	506	DNDG
28	Both sensitivity tests fail	**7.7**	**5.9**	No	0	Total Fissile
29		52.8	67.5	**Yes**	752	DNDG
30	Both sensitivity tests fail	**11.9**	**12.4**	No	0	Total Fissile
31		57.2	65.4	**Yes**	755	DNDG
32		51.3	56.6	**Yes**	564	DNDG
33		32.7	39.5	**Yes**	369	DNDG
34	Sample not analyzed	—	—	N/A	122	Total Fissile
35		29.6	24.3	**Yes**	246	DNDG
36	Both sensitivity tests fail	**9.2**	**8.4**	No	0	Total Fissile
37		17.2	16.2	**Yes**	73	DNDG
38	U sensitivity test fails	**9.5**	14.3	**Yes**	0	Total Fissile
39		14.1	16.5	**Yes**	48	DNDG
40		44.1	22.6	**Yes**	0	Total Fissile
41		19.1	24.6	**Yes**	122	DNDG

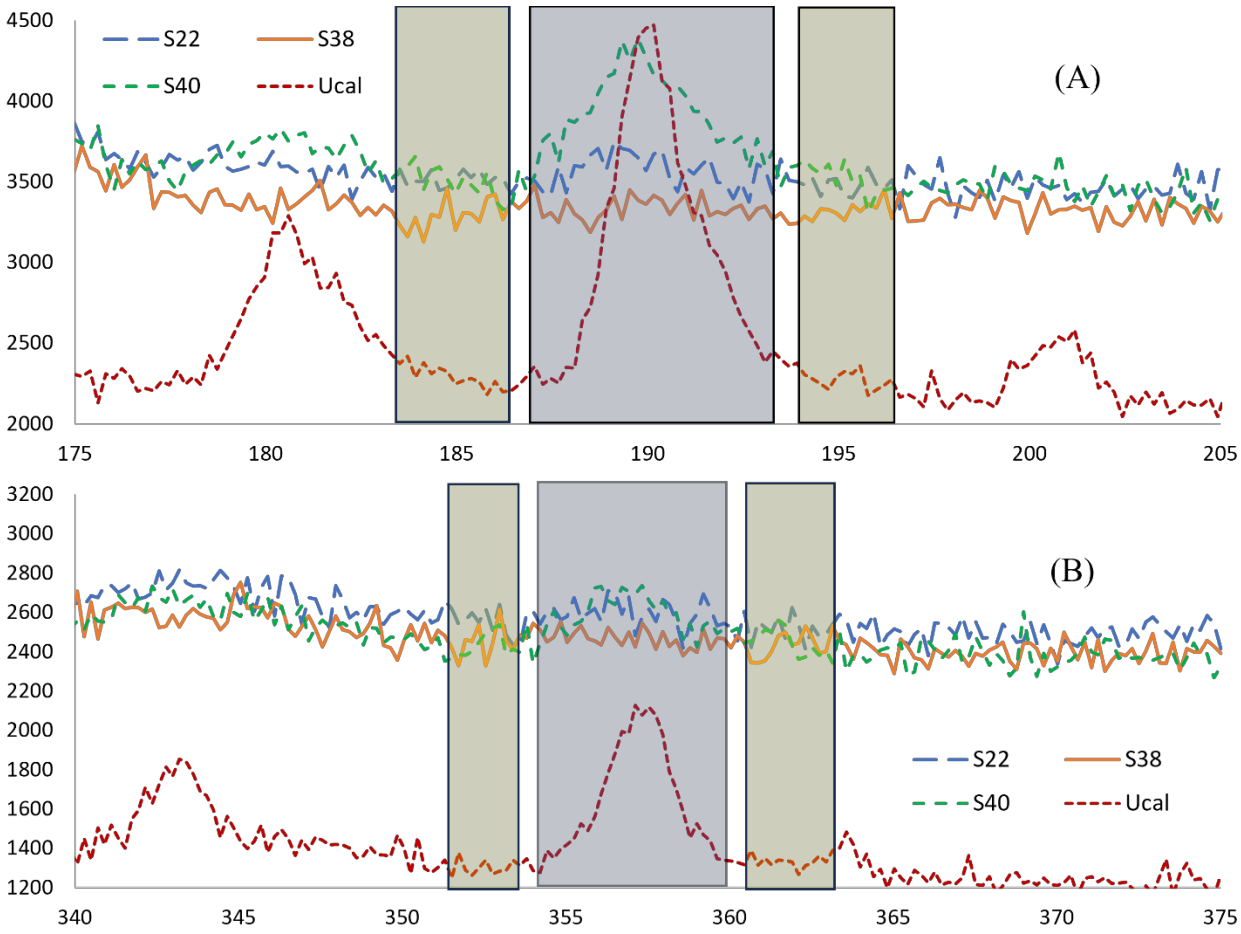

Figure 4. Comparison of 5 ng U calibration and field samples 22, 38, and 40. Panel (A) compares the 191 keV peak of ^{141}Ba, a marker for U. Panel (B) shows the 356 keV peak which can indicate ^{239}Pu presence. The ROI areas are marked for both peaks and the background areas beside them. The increased baseline and worsening peak resolution likely stem from higher count rates caused by sodium contamination in the stock solution used to prepare the field samples. However, false positive identification of Pu in sample 40 but not in sample 38 seems to result simply from statistics because the two spectra are very similar.

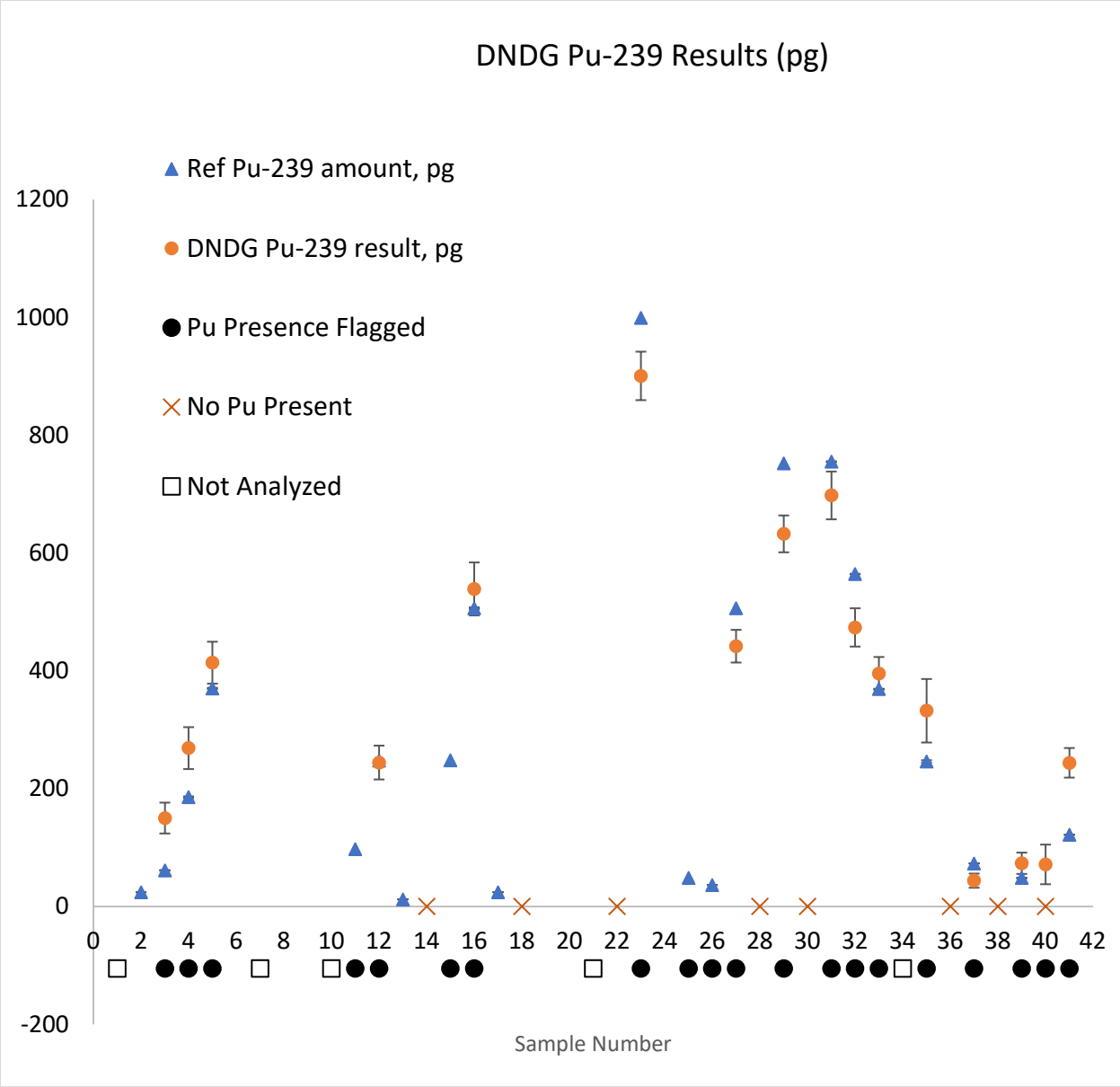

Figure 5. The measured Pu data are plotted against the true (reference) Pu mass loading. All of these values are calculated according to the DNDG method of gamma peak ratios. Samples containing no Pu are noted (X) along with the samples that were flagged for the presence of Pu by DNDG (●). Note that sample 12 has a high degree of overlap between the recipe Pu and measured Pu values and appears as a single point. Samples that were analyzed only by DN are designated by (□).

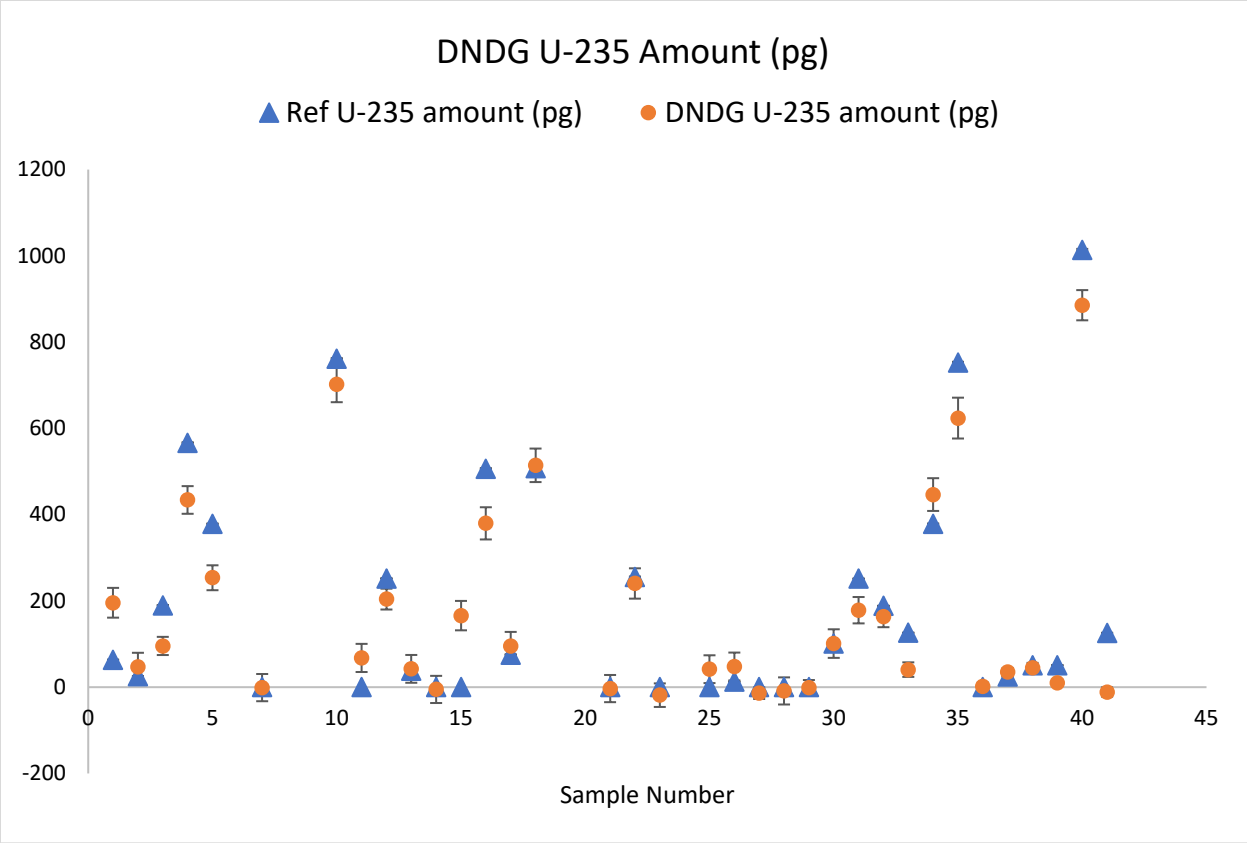

425

426 **Figure 6. The final U data are plotted against the true (reference) U mass loading.** Note that the
427 measured DNDG uranium values are a mixture of DN-only values for cases in which the peak sensitivity
428 test failed for either the 190 or 358 keV peaks. The remainder of the values are calculated by parsing the
429 DN data into Pu and U bins based on the gamma peak ratios.

430